Talanta 115 (2013) 271–276

Contents lists available at SciVerse ScienceDirect

Talanta

journal homepage: www.elsevier.com/locate/talanta

A novel europium-sensitive fluorescent nano-chemosensor based on new functionalized magnetic core–shell Fe_3O_4@SiO_2 nanoparticles

Mohammad Reza Ganjali [a], Morteza Hosseini [b,*], Mehdi Khobi [c], Shima Farahani [a], Masoom Shaban [a], Farnoush Faridbod [a], Abbas Shafiee [c], Parviz Norouzi [a]

[a] Center of Excellence in Electrochemistry, Faculty of Chemistry, University of Tehran, Tehran, Iran
[b] Department of Life Science Engineering, Faculty of New Sciences & Technologies, University of Tehran, Tehran, Iran
[c] Department of Medicinal Chemistry, Faculty of Pharmacy and Pharmaceutical Sciences Research Center, Tehran University of Medical Sciences, Tehran 14176, Iran

ARTICLE INFO

Article history:
Received 17 January 2013
Received in revised form
1 April 2013
Accepted 5 April 2013
Available online 30 April 2013

Keywords:
Nano-chemosensor
Fluorescence
Magnetic core–shell silica nanoparticles
Europium

ABSTRACT

A novel Eu^{3+}-sensitive fluorescent chemosensor is introduced. It is based on magnetic core–shell silica nanoparticle which is functionalized by Cinchonidine (CD-Fe_3O_4@SiO_2). The nano-chemosensor was synthesized and characterized by Fourier transform infrared spectroscopy (FT-IR), thermal gravimetric analysis (TGA), transmission electron microscopy (TEM), scanning electron microscopy (SEM), UV–visible absorption and fluorescence emission. The fluorescent nano-chemosensor shows a selective interaction with Eu^{3+} ion. Fluorescence studies revealed that the emission intensity of the functionalized magnetic core–shell silica nanoparticles (CD-Fe_3O_4@SiO_2 NPs) increases significantly by addition of various concentrations of Eu^{3+} ion. While in case of mono, di, and other trivalent cations, weak changes or either no changes in intensity were observed. The enhancement in fluorescence intensity of nano-chemosensor is because of the strong covalent binding of Eu^{3+} ion to CD-Fe_3O_4@SiO_2 NPs with a large binding constant value of 1.7×10^5 mol L^{-1}.

1. Introduction

Lanthanide series are becoming very important in different industries and even in biology. Lanthanide series are used in the production of glass and ceramic industries, metallurgy, electronics, agriculture and natural sciences [1,2]. Europium (Eu) is one of the lanthanide members, which can be applied in many areas of industries. Europium compounds play an important role in industries because of their special photogenic, magnetic, mechanical and nuclear properties. For example, they are used as a fluorescent agent in anodic rays of television and monitor screens.

The quantity determination of lanthanide family elements is one of the greatest problems in analytical chemistry, due to the close similarity of their chemical properties [3,4]. Today, there are some methods for determination of europium ions including, neutron activation analysis [5], luminescence enhancement method [6], spectrophotometric determination [7,8], voltammetry [9], laser-induced breakdown spectroscopy [10], inductively coupled plasma atomic emission spectrometry [11] and potentiometric sensor [12]. However, most of these methods often suffer from high cost, need to the large size of samples and inability for continuous monitoring.

Thus, developments of fluorescent sensors have attracted more attentions because they offer advantages of sensitivity, selectivity, response time and remote sensing [13–18].

Magnetic core–shell Fe_3O_4@SiO_2 nanoparticles, as special immobilizing carrier of bio-molecules, have aroused great interest in the current researches. They are biocompatible, easily renewable, and stable against degradation [19,20]. The inner iron-oxide core with outer shell of silica not only stabilizes the nanoparticles in the solution but also provides sites for surface modification by various biological ligands for biomedical applications [21].

Usually, inert silica coated on the surface of the magnetic nanoparticles prevents their aggregation in the solution. Thus, it improves their chemical stability, and provides better protection against toxicity [22]. In particular, the magnetic nanoparticles can also provide efficient binding to the guest molecules because their high surface-to-volume ratio simply offers more contact area [23].

Finding new type of fluorescent carriers, having excellent analytical characteristics, is of considerable interest. For instance, Schiff's base derivatives have been investigated in our laboratory as new type of fluorophores for optical chemosensing [24,25].

Readily accessible *cinchona alkaloids,* one of the important unique families of natural products, has numerous applications in pharmaceuticals, 'Privileged' type organocatalysts, resolving

* Corresponding author. Tel.: +98 2161118499; fax: +98 21 66495291.
E-mail address: smhosseini@khayam.ut.ac.ir (M. Hosseini).

0039-9140/$ - see front matter © 2013 Elsevier B.V. All rights reserved.
http://dx.doi.org/10.1016/j.talanta.2013.04.010

agents, NMR discriminating agents and chiral selectors in enantioselective analytical applications. They are commercially available, relatively inexpensive, stable, and environmentally harmless and their structure can be easily modified for diverse applications [26–31].

Here, we synthesized a novel organic–inorganic hybrid fluorescent nano-chemosensor for detection of Eu^{3+} ion. It was fabricated by covalently anchoring Cinchonidine (CD) to the surface of the silica gel encapsulated on Fe_3O_4 magnetite nanoparticles (denoted as [CD-Fe_3O_4@SiO_2]).

2. Experimental section

2.1. Materials

All chemicals were of reagent–grade from Fluka and Merck chemical companies. The nitrate and chloride salts of all the used cations were of the highest purity available and used without any further purification except for vacuum drying over P_2O_5. Tetraethylorthosilicate (TEOS), 3-mercaptopropyltrimethoxysilane (3-MPTMS) and Cinchonidine were also purchased from Merck Company. Other reagents and solvents were of analytical grade and used as received.

2.2. Instruments and spectroscopic measurements

IR spectra were taken using a Nicolet FT-IR Magna 550 spectrographs (KBr disks) (Nicolet, Madison, WI, USA) within 4000–400 cm^{-1}. SEM analysis was performed on a Philips XL-30 field-emission scanning electron microscope operated at 16 kV while TEM was carried out on a Tecnai G2 F30 at 300 kV. The experiments were performed using a microwave oven (ETHOS 1600, Milestone) with a power of 600 W specially designed for an organic synthesis and modified with a condenser and mechanical stirrer. The TGA thermo grams were obtained from a PL-Thermal science PL-STA 1500 instrument. The emission spectra were obtained on a Perkin-Elmer LS50 luminescence spectrometer. Fluorescence measurements were done in a 1 cm quartz cuvette containing a magnetic-stirred suspension of CD-Fe_3O_4@SiO_2 (20 mg L^{-1}) in 3 mL of aqueous medium EtOH/H_2O (30/70). This solution was titrated with standardized Eu^{3+} ion solution and the fluorescence intensity of the system was measured. The emission intensity was measured at an excitation wavelength of 330 nm. Spectral bandwidths of the monochromators for excitation and emission were 5 nm.

2.3. Preparation of Fe_3O_4@SiO_2-SH

Fe_3O_4 nanoparticles were synthesized via the co-precipitation of Fe^{2+} and Fe^{3+} ions (molar ratio 1:2) in alkali solution. $FeCl_3 \cdot 6\,H_2O$ (3.7 mmol) and $FeCl_2 \cdot 4\,H_2O$ (1.85 mmol) were dissolved in 30 mL deionized water and the resulting solution was dropped to a 25% NH_4OH solution (10 mL) with precisely constant drop rate under nitrogen gas and vigorous mechanical stirring (800 rpm) to obtain small and uniform particles. A black precipitate of Fe_3O_4 was continuously stirred for 1 h at room temperature and then heated to 80 °C for 2 h. The resulted Fe_3O_4 was collected by a permanent magnet after washing three times with deionized water and EtOH. Then, it was dried at 100 °C in vacuum for 24 h. A sample of obtained Fe_3O_4 (1 g) was suspended thoroughly in methanol (80 mL) by ultrasonic bath for 1 h at 40 °C. Then, concentrated ammonia solution was added to the resulting mixture and stirred at 40 °C for 30 min. Afterward, tetraethyl orthosilicate (TEOS, 1.0 mL) was introduced to the reaction vessel, and continuously stirred at 40 °C for 24 h. The silica-coated magnetic nanoparticles were separated by a permanent magnet, followed by washing several times with EtOH, diethyl ether and drying at 60 °C in vacuum for 24 h. In the next step, sample of silica coated magnetic nanoparticle (500 mg) was dispersed in anhydrous toluene with constant stirring under nitrogen atmosphere. After adding 3-mercaptopropyltrimethoxysilane (3-MPTMS, 1.0 mL) into the dispersed solution, the mixture was stirred for 1 day and the solid (Fe_3O_4@SiO_2-Si-$(CH_2)_3$-SH) was separated, washed with dry toluene and dried in vacuum for 24 h at room temperature. The solid (–SH) was separated, washed several times with dry toluene, MeOH, acetone and dried at 60 °C in vacuum for 24 h.

2.4. Preparation of CD-Fe_3O_4@SiO_2

To a 500 mg of synthesized Fe_3O_4@SiO_2-Si-$(CH_2)_3$-SH, which was thoroughly suspended in dry $CHCl_3$ (50 mL) by ultrasonic bath, 1 mmol Cinchonidine and 0.5 mmol α,ά-azoisobutyronitrile (AIBN) was added. After stirring at reflux for 48 h under Ar gas, the mixture was cooled to the room temperature, and separated by external magnet, then thoroughly washed with MeOH and $CHCl_3$, and dried in vacuum to give Cinchonidine bonded to the solid surface.

3. Results and discussion

CD-Fe_3O_4@SiO_2 was synthesized according to the procedure shown in Scheme 1. To confirm the surface modification of the CD-Fe_3O_4@SiO_2, NMR technique could not be used because of the super paramagnetic nature of catalyst's core. Hence, core–shell magnetic nanocrystallite CD-Fe_3O_4@SiO_2 were characterized by FTIR, SEM, TEM and TGA. The infrared (IR) spectra of Fe_3O_4@SiO_2 (Fig. 1a) and CD–Fe_3O_4@SiO_2 (Fig. 1b) are shown in Fig. 1.

Both spectra showed the presence of a Fe–O stretching vibration at approximately 632 cm^{-1}, an O–H stretching vibration due to the physisorbed water and potentially surface hydroxyls near 3442 cm^{-1}, and an O–H deformation vibration near 1626 cm^{-1}. The band at 1000–1300 cm^{-1} of the both samples is described to the Si–O stretching vibration on silanol [32]. Additionally, the most important asymmetric and symmetric C–H stretching bands are found at 2850 and 2925 cm^{-1} respectively, which prove successful bonding of alkyl moiety on silica coated magnetic nanoparticles. A weak band at 1428 cm^{-1} in Fig. 1a and b can also be correlated to the presence of CH_2 groups. The absorption bands at 1405–1460 cm^{-1} and 1626 cm^{-1} attributed to the characteristic absorption and flexural vibration of aryl group in appended organic moieties. It might have overlapped with the broad peaks due to

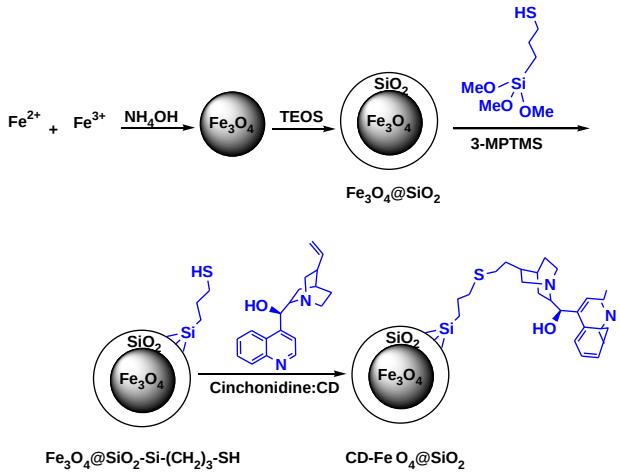

Scheme 1. synthesis route of CD-Fe_3O_4@SiO_2.

the silica coating and the bending mode of water molecules. The FTIR spectrum of the CD-Fe_3O_4@SiO_2 (Fig. 1b) shows new band at 1510 cm^{-1} and changes in the broad band at 1405–1460 cm^{-1} which is not pronounced in Fig. 1a and it can be correlated to the presence of CD group. Also spectrum 1a shows a kink on the curve near 3000 cm^{-1} due to the aromatic =C–H stretching, which may correspond to the aromatic ring originating of quinoline ring in Cinchonidine, representing the tethered Cinchonidine with Fe_3O_4@SiO_2–Si–$(CH_2)_3$–SH [33].

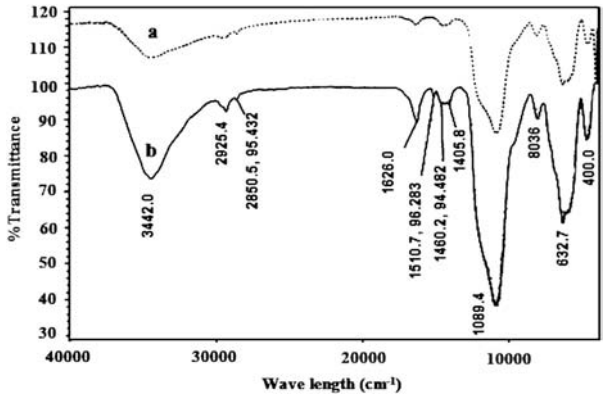

Fig. 1. IR spectra of (a) CD-Fe_3O_4@SiO_2, (b) Fe_3O_4@SiO_2.

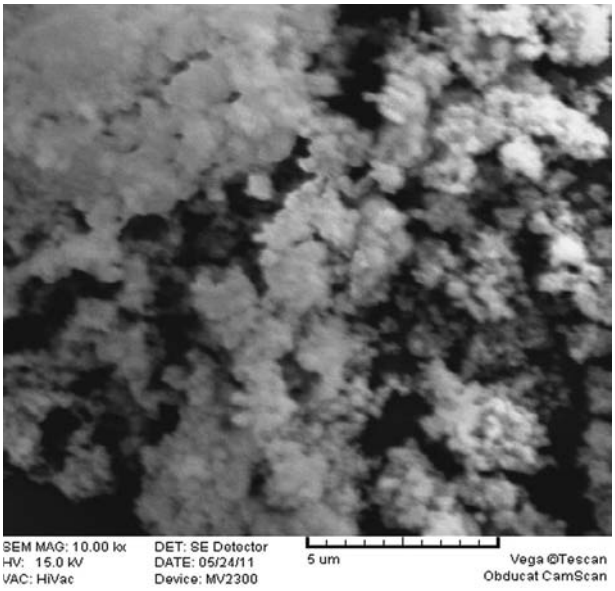

Fig. 2. SEM image of CD-Fe_3O_4@SiO_2.

SEM (Fig. 2) and TEM (Fig. 3) images showed that the average size of synthesized encapsulated nanoparticles is less than 30 nm and they present as uniform particles.

Quantitative determination of the functional group contents of the surface-bonded [CD-Fe_3O_4@SiO_2] nanocrystallites was performed using thermo-gravimetric analysis (TGA) and a loading of 0.16 ± 0.01 mmol g^{-1} of organic part was obtained (Fig. 4).

As shown in Fig. 4, TGA curve for CD-Fe_3O_4@SiO_2 have three temperature regions:

The first peak centered at 95 °C is due to the desorption of physically adsorbed water and dehydration of strongly associated water from the sample. The second temperature range from 200 to 400 °C is due to the decomposition of tethered Cinchonidine which seems to overlap the third temperature region between 400 and 600 °C [32]. The weight loss calculated from Fig. 4 in the temperature range of 400–600 °C is 2%, which means 0.07 ± 0.01 mmol g^{-1} of Cinchonidine is incorporated within functionalized Fe_3O_4@SiO_2, as illustrated in Scheme 1.

3.1. Preliminary studies

To consider whether CD–Fe_3O_4@SiO_2 can be used as a selective fluorescent chemosensor or not,, the variety of fluorescence spectra were obtained after addition of increasing amount of cations (1×10^{-4} mol L^{-1}) to an aqueous medium of the ligand (0.02 g L^{-1} of CD-Fe_3O_4@SiO_2 in EtOH/H_2O, 30/70) at 25.0 ± 0.1 °C. The resulting fluorescence intensity is shown in Fig. 5.

As shown in Fig. 5, the intensity of the emission band at 375 nm is enhanced by addition of Eu^{3+} ions. Other metal ions revealed no such increase in the emission band under the same conditions.

3.2. UV–vis titration

The cation binding properties of the ligand were investigated by UV–vis absorption spectroscopy too. Fig. 6 shows the absorption band of CD-Fe_3O_4@SiO_2 in ethanol/water solution (30/70: v/v) at 270 nm.

In this graph, the absorption intensity of CD-Fe_3O_4@SiO_2 at 270 nm gradually decreases as the concentration of Eu^{3+} increases stepwise. In addition, there were a well-defined isobestic points at 226 nm, respectively, it indicates that a stable complex with a

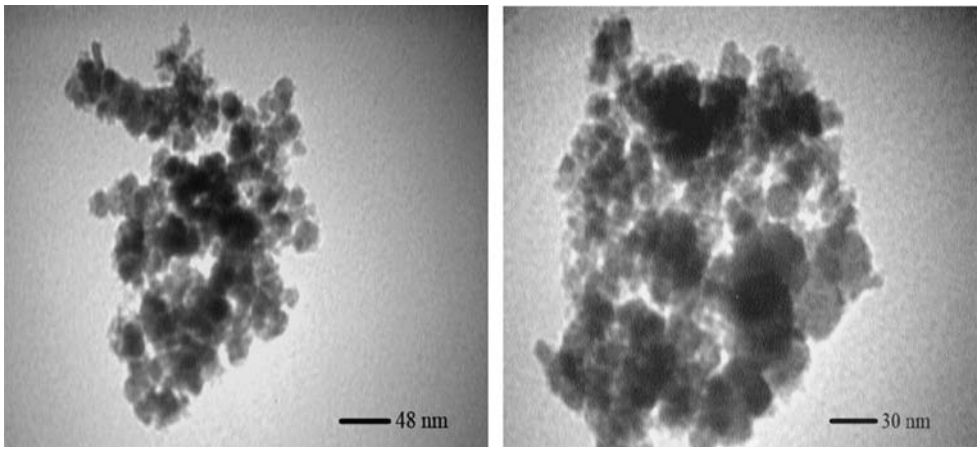

Fig. 3. TEM image of CD-Fe_3O_4@SiO_2.

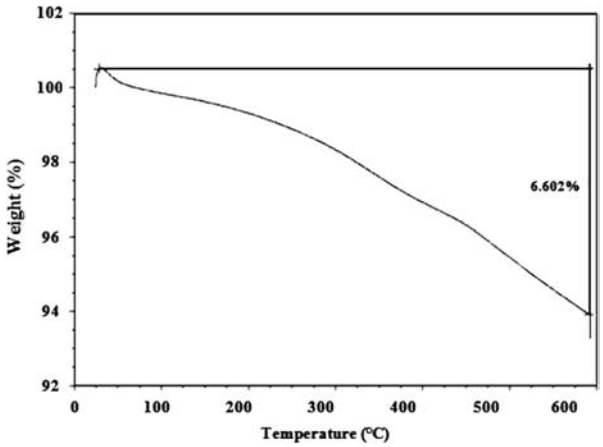

Fig. 4. TGA spectra of CD-Fe_3O_4@SiO_2.

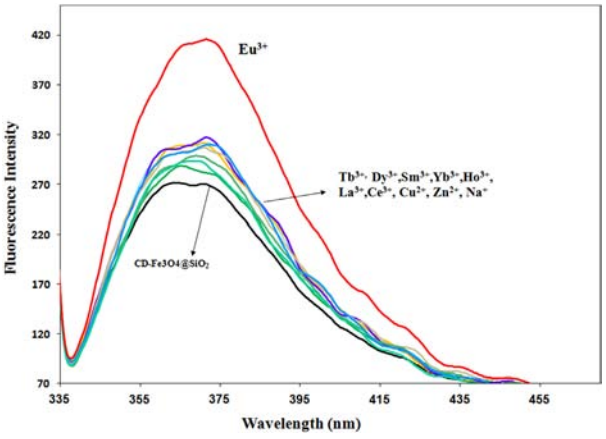

Fig. 5. Fluorescence emission spectra of CD-Fe_3O_4@SiO_2 (3 ml 0.8 mg L^{-1}) suspended in aqueous solution in the presence of different metal ions (1.0×10^{-4} mol L^{-1}). Excitation was performed at 360 nm.

certain stoichiometric ratio formed between the receptor CD-Fe_3O_4@SiO_2 and Eu^{3+} ion.

3.3. Fluorescence titrations

All of the fluorescence titration experiments were performed in a suspended aqueous solution and the maximum excitation wavelength was selected 330 nm. As illustrated in Fig. 7, CD-Fe_3O_4@SiO_2 showed a typical emission band around 375 nm, which was considerably enhanced in the presence of Eu^{3+} ion.

This phenomenon can be explained by photo-induced electron transfer (PET) mechanism [34,35]. By increasing the amounts of Eu^{3+} ion up to 2.0×10^{-6} mol L^{-1}, CD-Fe_3O_4@SiO_2 showed a large CHEF (chelation-enhanced fluorescence) effect in the emission spectra (more than 80%) which is the result of the blocking of the PET process (Fig. 7).

The detection limit of CD-Fe_3O_4@SiO_2 as a fluorescent sensor for the analysis of Eu^{3+} was studied from the plot of the fluorescence intensity as a function of the concentration of added cations. It was found that CD-Fe_3O_4@SiO_2 has a detection limit of 5.0×10^{-9} mol L^{-1} for Eu^{3+} ions in the linear range of 2.3×10^{-7} mol L^{-1}–3.6×10^{-6} mol L^{-1} [36].

The binding constant value has been determined from the fluorescence emission intensity data by the modified Benesi–Hildebrand equation [37,38]:

$$1/\Delta F = 1/\Delta F_{max} + (1/K[C])\,(1/\Delta F_{max})$$

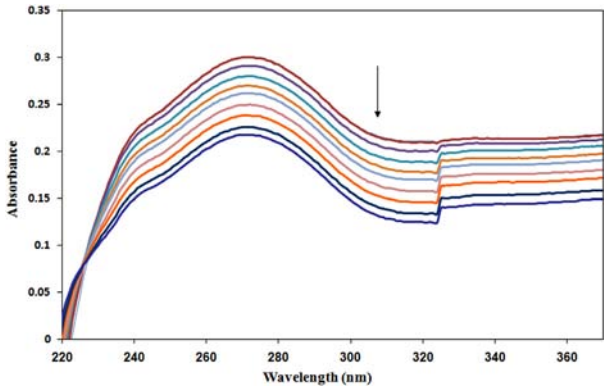

Fig. 6. Changes in the UV–vis spectra of CD-Fe_3O_4@SiO_2 (3 ml 0.1 gr L^{-1}) upon addition of Hg^{2+} (1.0×10^{-3} mol L^{-1}) in aqueous solution.

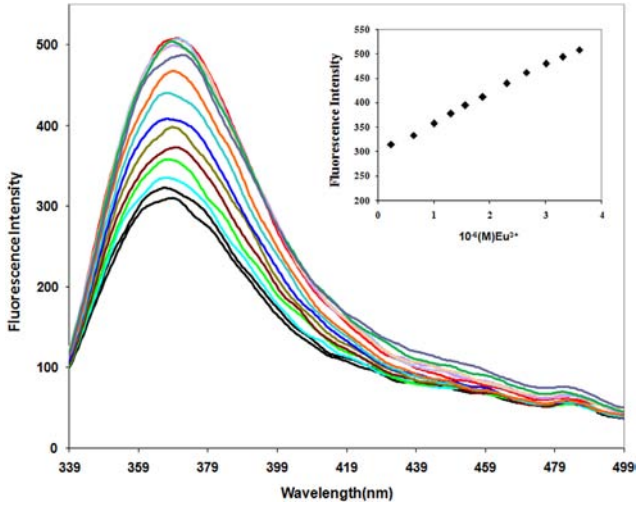

Fig. 7. Emission spectra of the proposed chemosensor in the presence of varying concentration of Eu^{3+} ions: (1) 0, (2) 2.3×10^{-7} mol L^{-1}, (3) 6.3×10^{-7} mol L^{-1}, (4) 1.0×10^{-6} mol L^{-1}, (5) 1.3×10^{-6} mol L^{-1}, (6) 1.6×10^{-6} mol L^{-1} (7) 2.0×10^{-6} mol L^{-1}, (8) 2.3×10^{-6} mol L^{-1}, (9) 2.6×10^{-6} mol L^{-1}, (10) 3.0×10^{-6} mol L^{-1}, (11) 3.3×10^{-6} mol L^{-1}, (12) 3.6×10^{-6} mol L^{-1}, λ_{ex}=330 nm.

Here, $\Delta F=F_x-F_0$ and $\Delta F_{max}=F_\infty-F_0$, where F_0, F_x, and F_∞ are the emission intensities of CD-Fe_3O_4@SiO_2 considered in the absence of Eu^{3+} ion, at the intermediate Eu^{3+} ion concentration and at the concentration of complete interaction, respectively, and where K is the binding constant and [C] the Eu^{3+} ion concentration. From the plot of $(F_\infty-F_0)/(F_x-F_0)$ against $[Eu^{3+}]^{-1}$, the value of K extracted from the slope is 1.7×10^5 mol L^{-1}.

A comparison between this work and other previous reported methods for Eu^{3+} ion determination is listed in Table 1. In comparison with these methods, the nano-chemosensor has a wider linear range than luminescence enhancement methods. The detection limit of the proposed nano-chemosensors is 5.0×10^{-9} mol L^{-1} which is lower than those of the neutron activation analyses, luminescence enhancement, spectrophotometric, ICP-AES, voltammetric and potentiometric methods. In term of the linear range and detection limit, it can be seen that the nano-chemosensor displays even more sensitivity than most of the reported methods [5–12].

3.4. Selectivity

The selectivity behavior is obviously one of the most important characteristics of a chemosensor, which is the relative response of the sensor to the primary ion presence of the other ions in the solution.

Table 1
Comparison of the linear range and detection limit (LOD) of several different methods for determination of Eu^{3+}.

Method	Linear range (mol L^{-1})	LOD (mol L^{-1})	Reference
Neutron activation analysis	–	2.1×10^{-5}	5
Luminescence enhancement method	4.0×10^{-6}–2.4×10^{-5}	4.3×10^{-6}	6
Spectrophotometry	6.5×10^{-7}–3.9×10^{-6}	6.5×10^{-8}	7
	0–1.16×10^{-6}	1.25×10^{-7}	8
Voltammetry	5.0×10^{-7}–3.0×10^{-5}	1.5×10^{-7}	9
Laser-induced breakdown spectroscopy	–	2.7×10^{-5}	10
ICP-AES	–	6.0×10^{-7}	11
Potentiometric sensor	1.0×10^{-6}–1.0×10^{-2}	4.0×10^{-7}	12
Fluorescent nano-chemosensor	2.3×10^{-7}–3.6×10^{-6}	5.0×10^{-9}	This work

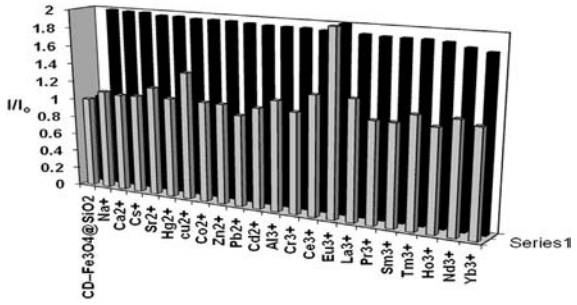

Fig. 8. (a) Gray bars represent relative fluorescence intensity of CD-Fe_3O_4@SiO_2 (20 mg L^{-1}) in the presence of various cations (5×10^{-6} mol L^{-1}) in the aqueous solution, λ_{ex}=330 nm, (b) Black bars represent relative fluorescence intensity of CD-Fe_3O_4@SiO_2 (20 mg L^{-1}) containing 5×10^{-6} mol L^{-1} cations and the background Eu^{3+} (5×10^{-6} mol L^{-1}) (λ_{ex}: 330 nm).

Table 2
Determination of Eu^{3+} in tap and river water samples.

Sample	Added Eu^{3+} (mg L^{-1})	Found(mg L^{-1}) [a]	Recovery (%)
Tap water	0.20	0.19 ± 0.02	95
	0.40	0.41 ± 0.01	102.5
River water	0.20	0.21 ± 0.03	105
	0.40	0.41 ± 0.01	102.5

[a] The results are based on 3 replicates.

To examine the selectivity of the proposed nano-chemosensor, we investigated its affinity for other metal ions, including all mono, di, and trivalent metal ions. The influence of the interfering ions such as Na^+, Cs^+, Ca^{2+}, Sr^{2+}, Cu^{2+},Zn^{2+}, Cd^{2+}, Hg^{2+}, Co^{2+}, Pb^{2+}, Al^{3+}, Cr^{3+}, La^{3+}, Ce^{3+}, Eu^{3+}, Pr^{3+}, $Sm3^+$ and Er^{3+} on the fluorescence behavior of CD-Fe_3O_4@SiO_2 (20 mg L^{-1}) was shown in Fig. 8.

As shown in Fig. 8 the results reveal that among the metal ions studied, only Eu^{3+} has a significant effect on the fluorescence intensity of CD-Fe_3O_4@SiO_2 (20 mg L^{-1}). Fluorescence enhancement of CD-Fe_3O_4@SiO_2 was observed upon the addition of excess other metal ions.

The competition measurements were carried out by the subsequent addition of 5×10^{-6} mol L^{-1} metal ions to the solution of CD-Fe_3O_4@SiO_2 in aqueous solution. The fluorescence spectra were recorded at 375 nm with the addition of these metal ions and the subsequent addition of (5×10^{-6} mol L^{-1}) Eu^{3+} to the above solutions. Also Fig. 8 illustrates that the enhancement in the fluorescence intensity resulting from the addition of Eu^{3+} ion has not been significantly influenced by addition of mono, divalent metal ions and other trivalent lanthanides series.

Consequently, the new hybrid material CD-Fe_3O_4@SiO_2 can be used as a chemosensor for the detection of different concentrations of Eu^{3+} ion with high selectivity.

3.5. Analytical application

The proposed method was applied for determination of europium content of tap water and river water samples, and the results of triplicate measurements are summarized in Table 2. The amount of the europium ions, which were added to the water samples (0.20–0.4 mg L^{-1}), could be determined by the sensor with relatively good accuracy.

4. Conclusion

In summary, magnetic core–shell Fe_3O_4@SiO_2 nanoparticles functionalized by CD was successfully designed and synthesized. It acts as a fluorescent chemosensor for detection of Eu^{3+} ion. This work provides a platform to report magnetic nanoparticles modified by organic fluorescent chemosensor with high affinity, selectivity and sensitivity to detect metal ions.

Acknowldegements

The authors are grateful to the Research Council of University of Tehran for the financial support of this work.

References

[1] D.R. Lide, CRC Handbook of Chemistry and Physics, 87th ed., CRC Press, Boca Raton, 2006 FL0-8493-0487-3.
[2] R.E. Kirk and D.F. Othmer, Encyclopedia of Chemical Technology, Interscience Publishers, a Division of John Wiley & Sons, New York-London vol. 19, 1982, Wiley, 851.
[3] V. Bekiari, P. Judeinstein, P.J. Lianos, Luminescence 104 (2003) 13–15.
[4] W.S.H. Xia, R.H. Schmehl, C.J. Li, Tetrahedron 56 (2000) 7045–7049.
[5] D.k. Tehrani, N. Badawi, J. Radioanal. Nucl. Chem. 136 (1989) 1–7.
[6] L. Zhang, X. Zheng, W. Ahmad, Y. Zhou, Y. An, Spectrochim. Acta Part A 104 (2013) 243–249.
[7] S. Liawruangrath, S. Sakulkhaemaruethai, Talanta 59 (2003) 9–18.
[8] Q.Z. Zhai, W.H. Hu, Y. Zhang, Instrum. Sci. Technol. 38 (2010) 201–209.
[9] T. Alizadeh, S. Amjadi, Talanta, Corrected Proof. Available from: 15, 2013,431–439, http://dx.doi.org/10.1016/j.talanta.2013.01.019, in press.
[10] E.C. Jung, D.H. Lee, J.I. Yun, J.G. Kim, J.W. Yeon, K. Song, Spectrochim. Acta A 66 (2011) 761–764.
[11] H. Mitsumata, I. Aoki, J. Ceram. Soc. Jpn. 112 (2004) 608–611.
[12] H.A. Zamani, R. Kamjoo, M. Mohammadhosseini, M. Zaferoni, Z. Rafati, M. R. Ganjali, F. Faridbod, Mater. Sci. Eng. C 32 (2012) 447–451.
[13] J.R. Lakowicz, Principles of Fluorescence Spectroscopy, Kluwer Academic, Plenum Publishers, New York, 1999.
[14] J.P. Desvergne, A.W. Czarnic (Eds.), Chemosensors for Ion and Molecule Recognition, Kluwer Academic Publishers, Dordecht, 1997.
[15] M.R. Ganjali, M. Hosseini, M. Hariri, F. Faridbod, P. Norouzi, Sens. Actuators B 142 (2009) 90–96.
[16] M.R. Ganjali, B. Veismohammadi, M. Hosseini, P. Norouzi, Spectrochim. Acta A 74 (2009) 575–578.
[17] M. Hosseini, Z. Vaezi, M.R. Ganjali, F. Faridbod, S. Dehghan Abkenar, Spectrochim. Acta A 83 (2011) 161–164.
[18] M. Hosseini, M.R. Ganjali, M. Tavakoli, P. Norouzi, F. Faridbod, H. Goldooz, A. Badiei, J. Fluoresc. 21 (2011) 1509–1513.
[19] C. Fang, M. Zhang, J. Mater. Chem. 19 (2009) 6258–6266.
[20] J. Gao, H. Gu, B. Xu, Acc. Chem. Res. 42 (2009) 1097–1107.

[21] K.H. See, M.E. Mullins, O.P. Mills, P.A. Heiden, Nanotechnol. 16 (2005) 1950–1959.
[22] A.I. Lesnikovich, T.M. Shunkevich, V.N. Naumenko, S.A. Vorobyova, M. V. Baykov, J. Magn. Magn. Mater. 85 (1990) 14–16.
[23] H.Y. Lee, D.R. Bae, J.C. Park, H. Song, W.S. Han, J.H. Jung, Angew. Chem. Int. Ed. 48 (2009) 1239–1243.
[24] M. Hosseini, Z. Vaezi, M.R. Ganjali, F. Faridbod, S. Dehghan Abkenar, K. Alizadeh, M. Salavati-Niasari, Spectrochim. Acta A 75 (2010) 978–982.
[25] M. Hosseini, Z. Vaezi, M.R. Ganjali, F. Faridbod, S. Dehghan Abkenar, M. Salavati-Niasari, Sensor Lett. 8 (2010) 807–812.
[26] K. Kacprzak, B. Gierczyk, Tetrahedron 21 (2010) 2740–2745.
[27] M. Xuebing, Y. Wang, W. Wang, J. Cao, Catal. Commun. 11 (2010) 401–407.
[28] H.S. Kim, Y.M. Song, J.S. Choi, J.W. Yang, H. Han, Tetrahedron 60 (2004) 12051–12057.
[29] N. He, F. Wang, C. Ma, C. Li, X. Zeng, Y. Deng, L. Zhang, Z. Li, J. Biomed. Nanotechnol. 9 (2013) 267–273.
[30] F. Wang, C. Ma, X. Zeng, C. Li, N. He, J. Biomed. Nanotechnol. 8 (2012) 786–790.
[31] H. Sun, X. Zeng, M. Liu, S. Elingarami, G. Li, B. Shen, N. He, J. Nanosci. Nanotechnol. 12 (2012) 267–273.
[32] X. Peng, Y. Wang, X. Tang, W. Liu, Dyes Pigm. 91 (2011) 26–32.
[33] S. Ghosh, A.Z.M. Badruddoza, M.S. Uddin, K. Hidajat, J. Colloid Interface Sci. 354 (2011) 483–492.
[34] B. Valeur, I. Leray, Coord. Chem. Rev. 205 (2000) 3–40.
[35] A. Prasanna de silva, D.B. Fox, A.J.M. Huxley, T.S. Moody, Coord. Chem. Rev. 205 (2000) 41–57.
[36] P. Bühlmann, E. Pretsch, E. Bakker, Chem. Rev. 97 (1997) 3083–3132.
[37] A. Mallick, N. Chattopadhyay, Photochem. Photobiol. 81 (2005) 419–424.
[38] H.A. Benesi, J.H. Hildebrand, J. Am. Chem. Soc. 71 (1949) 2703–2707.